Iranian Journal of Oil & Gas Science and Technology, Vol. 8 (2019), No. 2, pp. 53-72
http://ijogst.put.ac.ir

A Numerical Simulation Study on the Kinetics of Asphaltene Particle Flocculation in a Two-dimensional Shear Flow

Hadi Bagherzadeh[1], Zahra Mansourpour[2], and Bahram Dabir[3*]

[1] Ph.D. Candidate, Petroleum Engineering Department, Amirkabir University of Technology, Tehran, Iran
[2] Assistant Professor, Chemical Engineering Department, University of Tehran, Tehran, Iran
[3] Professor, Petroleum Engineering Department, Amirkabir University of Technology, Tehran, Iran

Received: August 31, 2018; *revised*: October 13, 2018; *accepted*: November 13, 2018

Abstract

In the current study, the kinetics of asphaltene particle flocculation is investigated under a shear flow through numerical simulation. The discrete element method (DEM) is coupled with computational fluid dynamics (CFD) to model the agglomeration and fragmentation processes. In addition, a coalescence model is proposed to consider the attachment of colliding particles. The changes in mean asphaltene floc size, the particle size distribution (PSD) of asphaltene flocs over simulation time, and the average fractal dimension are presented. Moreover, the effect of fluid velocity on the kinetics of asphaltene flocculation is examined. The mean asphaltene floc size increases exponentially at first, and then the growth slows; finally, it ceases due to the establishment of a dynamic equilibrium between the agglomeration and fragmentation processes. As expected, asphaltene PSD's move from fine to coarse sizes during the simulation. Log-normal distribution matches the PSDs best, which is in agreement with the nature of asphaltene. As fluid velocity increases, the dynamic equilibrium is attained more rapidly at a smaller mean floc size and higher average fractal dimension; furthermore, PSDs shift to smaller asphaltene floc sizes. The obtained average fractal dimensions of the asphaltene flocs are in the range of 1.65 to 1.74, which is compatible with the values reported in the literature. Eventually, a semi-analytical model is utilized to fit the simulation results. It is found out that the semi-theoretical model is capable of predicting the evolution of asphaltene particle size appropriately.

Keywords: Asphaltene Flocculation, Kinetics, Discrete Element Method, Computational Fluid Dynamics

1. Introduction

Asphaltene is known as the cholesterol of petroleum since its precipitation and deposition can cause serious problems during oil production, transportation, and processing (Kokal et al., 1995). Changes in pressure, temperature, and the composition of crude oil may lead to asphaltene precipitation. The precipitated asphaltene particles (known as primary particles) tend to flocculate, and asphaltene flocs will subsequently be formed. Then, the asphaltene flocs can deposit along oil production systems. The investigation of the asphaltene deposition in the wellbore and flowlines has received special attention

* Corresponding Author:
Email: drbdabir@aut.ac.ir

in recent decade (Ramirez-Jaramillo et al., 2006; Jamialahmadi et al., 2009; Vargas et al., 2010; Eskin et al., 2011; Shirdel et al., 2012; Haghshenasfard et al., 2015; Fallahnejad et al., 2016; Seyyedbagheri et al., 2017; Salimi et al., 2017). The size of asphaltene flocs is a key factor in asphaltene deposition behavior. Hence, the investigation of the kinetics of asphaltene flocculation has attracted a lot of attention in the literature. The size and morphology of asphaltene flocs have been studied using different techniques, including small-angle neutron and X-ray scattering (Savvidis et al., 2001; Mason and Lin, 2003; Headen et al., 2009; Eyssautier et al., 2011), a combination of viscosimetric and neutron scattering measurement (Fenistein et al., 1998; Sheu et al., 2007; Hoepfner et al., 2013), optical microscopy (Rahmani et al., 2005), and particle size analyzer (Ferworn et al., 1993; Rastegari et al., 2004; Daneshvar, 2005). These studies have shown asphaltene flocs with sizes ranging from tens to hundreds of micrometers, which have loose fractal-like structures with fractal dimensions varied from 1.06 to 2. Also, the agglomeration and fragmentation of asphaltene particles in model oil mixtures have been investigated under a laminar flow condition using Taylor-Couette device (Rahmani et al., 2003 and 2004; Solaimany-Nazar and Rahimi, 2008 and 2009). These results have indicated that the asphaltene flocs grow to average diameters in the order of 100 micrometers. Moreover, a maximum in the average asphaltene floc diameter is observed at intermediate time scales followed by a decrease in the mean floc size during asphaltene particle evolution.

The most of researchers studied the kinetics of asphaltene flocculation used population balance equations (PBE's) to describe the growth of precipitated asphaltene particles and predict particle size distribution (Rahmani et al., 2003; Solaimany-Nazar and Rahimi, 2008; Khoshandam and Alamdari, 2010; Maqbool et al., 2011; Eskin et al., 2011; Mohammadi et al., 2016). PBE's take the birth and death of different-sized classes of asphaltene flocs into account as a result of agglomeration and fragmentation processes. PBE's calculations need the rate constants for both aforementioned processes, called kernels. The kernels are a function of the floc size, floc structure, the applied shear rate, and interparticle interactions. The determination of these kernels requires an in-depth understanding of the underlying physics of the corresponding processes. Recently, the agglomeration and fragmentation of asphaltene flocs have been studied in turbulent flows using an Eulerian-Lagrangian approach by Schutte et al. (2015). Their results have indicated that, in the course of asphaltene evolution, very open and porous asphaltene flocs are formed, and their properties show little dependency to Reynolds number and fragmentation mechanisms. The chemical properties of asphaltenes have not been considered in this work. It seems studying the kinetics of asphaltene flocculation on the level of individual particles needs more attention and can provide a deep insight into the physics behind the agglomeration and fragmentation processes.

The present paper considers the evolution of precipitated asphaltene particles numerically using discrete element method-computational fluid dynamics (DEM-CFD) approach under a laminar flow condition. DEM predicts asphaltene particle collisions and the corresponding contact forces, and CFD is used to calculate the flow field. The attachment of colliding particles is taken into account by a proposed coalescence model according to the nature of asphaltene. Additionally, the fragmentation of asphaltene flocs due to hydrodynamic forces is also implemented in the simulation. The mean asphaltene floc size and the particles size distribution of flocs are presented during simulation along with an average fractal dimension of asphaltene flocs. Moreover, the effect of fluid velocity on the kinetics of asphaltene flocculation is investigated. Finally, a semi-theoretical model proposed by Chimmili et al. (1998) is used to fit mean asphaltene floc size resulted from the simulation.

2. Theory

2.1. Numerical model

In the present work, numerical simulation has been carried out in a 2D channel flow as thick as a primary particle diameter under a laminar flow condition where Reynolds number varies in the range of 310-630 in the simulation runs. To this end, an in-house code has been developed in FORTRAN to investigate the kinetics of asphaltene particle flocculation using a DEM-CFD approach. In the following, the governing equations of the continuous and discrete phases as well as coalescence and fragmentation models are presented.

a. Governing equations of the continuous and discrete phases

The governing equations, including the continuity and momentum balance for oil as continuous phase in the presence of asphaltene particles are presented in Equations 1 and 2 respectively (Anderson and Jackson, 1967):

$$\frac{\partial \varepsilon}{\partial t} + \nabla.(\varepsilon U_f) = 0 \tag{1}$$

$$\frac{\partial (\rho_f \varepsilon U_f)}{\partial t} + \nabla.\left(\rho_f \varepsilon U_f U_f\right) = -\nabla P - F^f{}_p + \nabla.(\varepsilon \tau) + \rho_f \varepsilon g \tag{2}$$

where, ρ_f, U_f, P, τ, and ε represent fluid density, fluid velocity, pressure, fluid viscous stress tensor, and porosity respectively. In Equation 2, viscous stress tensor has been considered to model shear stresses in the continuum phase (oil phase).

In the aforementioned equations, ε is computed based on the area occupied by the particles in each fluid cell in a 2D simulation domain:

$$\varepsilon_{2D} = 1 - \frac{1}{A_{Cell}} \sum_{i=1}^{N} \alpha_p^i A_p \tag{3}$$

2D porosity should be converted to 3D porosity when it is used in correlations used for calculating the drag force. Accordingly, Equation 4 suggested by Hoomans et al. (1996), has been applied:

$$\varepsilon_{3D} = 1 - \frac{2}{\sqrt{\pi\sqrt{3}}} (1 - \varepsilon_{2D})^{3/2} \tag{4}$$

The forces exerted on the particles can be divided into two categories, including particle-particle contact forces and particle-fluid interaction forces. The contact forces as a result of particle-particle and particle-wall interactions are computed using soft-sphere method as one of the approaches in DEM modeling. The equations related to normal and tangential contact forces based on linear spring-dashpot model are embedded in Table 1 (Cundall and Strack, 1979). Moreover, the drag forces are considered to account for the fluid–particle interactions. The equations proposed by Ergun (1952) and Wen and Yu (1966) are used to calculate the drag forces acting on a primary particle as presented in Table 1. The drag force acting on a floc is determined by the summation of the drag forces on its constituent primary particles. In addition, the dispersed phase exerts a force on the continuous phase which equals the fluid force acting on the dispersed phase but in the opposite direction because of the assumption of two-way coupling in the simulation. It should be noted that since the equations

presented for the calculation of drag force are related to force acting on asphaltene primary particles, there is no need to refine fluid cells as asphaltene flocs grow over time.

Table 1

Equations used to calculate contact forces and drag force.

Term	Equation
Normal contact force	$\vec{F}^{n}{}_{cont,ij} = \left(-k_n \xi_{n,ij} - \eta_n (\vec{v}_{ij}.\vec{n}_{ij})\right) \vec{n}_{ij}$
Tangential contact force	$\vec{F}^{t}{}_{cont,ij} = \begin{cases} \left(-k_t \xi_{t,ij} - \eta_t (\vec{v}_{ij}.\vec{t}_{ij})\right)\vec{t}_{ij}, & \left\|\vec{F}^{t}{}_{cont,ij}\right\| \le \mu_p \left\|\vec{F}^{n}{}_{cont,ij}\right\| \\ -\mu_p \left\|F^{n}{}_{cont,ij}\right\| \vec{t}_{ij}, & \left\|\vec{F}^{t}{}_{cont,ij}\right\| > \mu_p \left\|\vec{F}^{n}{}_{cont,ij}\right\| \end{cases}$
Normal overlap	$\xi_{n,ij} = \left(R_i + R_j\right) - \left\|\vec{r}_i - \vec{r}_j\right\|$
Normal unit vector	$\vec{n}_{ij} = \dfrac{(\vec{r}_i - \vec{r}_j)}{\left\|\vec{r}_i - \vec{r}_j\right\|}$
Relative velocity	$\vec{v}_{ij} = \left(\vec{v}_i - \vec{v}_j\right) + (\vec{\omega}_i \times \vec{R}_i - \vec{\omega}_j \times \vec{R}_j)$
Tangential overlap	$\xi_{t,ij} = \xi_{t0,ij} + (\vec{v}_{ij}.\vec{t}_{ij})\Delta t_p$
Drag force	$\begin{cases} \vec{f}_i = V_p \left(150 \dfrac{(1-\varepsilon)^2 \mu_f}{\varepsilon {D_p}^2} + 1.75 \dfrac{\rho_f (1-\varepsilon)\left\|\vec{U}_f - \vec{v}_p\right\|}{D_p}\right)(\vec{U}_f - \vec{v}_p) & , \varepsilon < 0.8 \\ \vec{f}_i = V_p \left(\dfrac{\pi}{8} C_D \varepsilon^{-2.65} \rho_f {D_p}^2 \left\|\vec{U}_f - \vec{v}_p\right\| (\vec{U}_f - \vec{v}_p)\right) & , \varepsilon \ge 0.8 \end{cases}$
Drag coefficient	$C_D = \begin{cases} \dfrac{24}{Re_p}\left(1 + 0.15 {Re_p}^{0.687}\right) & , Re_p < 1000 \\ 0.44 & , Re_p \ge 1000 \end{cases}$
Reynolds number	$Re_p = \dfrac{\rho_f \varepsilon D_p \left\|\vec{U}_f - \vec{\upsilon}_p\right\|}{\mu_f}$

The translational and rotational motions of asphaltene particles including primary particles and flocs are described as follows (Xu and Yu, 1997):

$$m_i \frac{d\vec{v}_i}{dt} = \vec{F}^{n}{}_{cont,i} + \vec{F}^{t}{}_{cont,i} + \vec{F}^{f}{}_{i} + m_i g \tag{5}$$

$$I_i \frac{d\omega_i}{dt} = \sum \vec{r}_{cont} \times \vec{F}^{t}{}_{cont} \tag{6}$$

where, v_i and ω_i are the translational and angular velocities of the asphaltene particle respectively. The involved forces are the normal and tangential contact forces ($\vec{F}^{n}{}_{cont,i}, \vec{F}^{t}{}_{cont,i}$), particle–fluid interaction force ($\vec{F}^{f}{}_{p}$), and finally the gravitational force.

To describe the motion of rigid asphaltene flocs, the multi-sphere method proposed by Kruggel-Emden et al. (2008) was used for representing irregular-shaped flocs within the DEM. To this end,

two frames of reference should be introduced: an inertial frame, which is not moving with the floc, and a body fixed frame, which is located in the center of the gravity of the floc. The translational motion of a floc is obtained from Newton's second law in the inertial frame, whereas its rotational motion obeys the Euler equations in the body fixed frame. For a floc composed of *N* primary particles, overall mass (m_F), center of gravity ($\vec{r}_{CGF}$), and inertial tensor (I_F) are computed as follows:

$$m_{\mathrm{F}} = \sum_{\mathrm{k}=1}^{\mathrm{N}} m_{pk} \tag{7}$$

$$\vec{r}_{CGF} = \frac{\sum_{\mathrm{k}=1}^{\mathrm{N}} m_{pk}\vec{r}_{pk}}{m_{\mathrm{f}}} \tag{8}$$

$$\hat{I}_F = \begin{bmatrix} \sum I_{pk} + \sum m_{pk}(y_{pk}^2 + z_{pk}^2) & -\sum m_{pk}x_{pk}\,y_{pk} & -\sum m_{pk}x_{pk}\,z_{pk} \\ -\sum m_{pk}x_{pk}\,y_{pk} & \sum I_{pk} + \sum m_{pk}(x_{pk}^2 + z_{pk}^2) & -\sum m_{pk}y_{pk}\,z_{pk} \\ -\sum m_{pk}x_{pk}\,z_{pk} & -\sum m_{pk}y_{pk}\,z_{pk} & \sum I_{pk} + \sum m_{pk}(x_{pk}^2 + y_{pk}^2) \end{bmatrix} \tag{9}$$

b. Coalescence model

The percentage of successful collisions (leading to agglomeration) depends on the magnitude of repulsive forces compared to attractive forces. Due to the lack of knowledge about these forces, the most challenging part of kinetic modeling of asphaltene flocculation is the establishment of a criterion for the attachment of colliding particles. In this work, an approach, based on a common energy balance proposed by Henry et al. (2013) in colloidal agglomeration, is adopted for the attachment of colliding asphaltene particles. In this approach, agglomeration happens if the relative kinetic energy of the pair of colliding particles ($E_{kin,\,ij}$) is high enough to overcome the repulsive forces (U_{bar}) between the particles, which are called energy barrier. $E_{kin,\,ij}$ is computed by:

$$E_{kin,ij} = \frac{1}{2}(m_i + m_j)(|\vec{v}_i - \vec{v}_j|)^2 \tag{10}$$

The magnitude of energy barrier should now be computed. According to the work of Haji-Akbari et al. (2013), the energy barrier is inversely related to the squared difference between the solubility parameters of asphaltenes and the solution as defined by Equation 11. On the other hand, collision efficiency (β) can be related to the energy barrier using Equation 12. Therefore, when the relation between collision efficiency and the difference between the solubility parameters is experimentally specified, the energy barrier can be calculated by Equation 13. In this equation, both C_1 and C_2 are constants.

$$U_{bar} \propto \frac{1}{\left(\delta_{asph} - \delta_{sol}\right)^2} \tag{11}$$

$$\beta = \exp(-\frac{U_{bar}}{K_B T}) \tag{12}$$

$$\frac{U_{bar}}{K_B T} = -\ln(\beta) = \frac{C_1}{\left(\delta_{asph} - \delta_{sol}\right)^2} + C_2 \tag{13}$$

c. Fragmentation model

The fragmentation of resultant asphaltene flocs can occur due to a hydrodynamic shear force. In this work, straining and shearing modes are considered in the fragmentation process. Straining and shearing are related to the normal and tangential components of the force exerted on the floc respectively (Schutte et al., 2015).

The following procedure is used for calculating the internal stresses. According to Equation 14, the accelerations of primary particles of a floc should obey the rigid-body equation of motion. Alternatively, the accelerations can result from a force balance acting on those primary particles. Thus, the force exerted by fluid on each bond between the primary particles of a floc is computed using Equation 15:

$$\frac{d\vec{v}_p}{dt} = \frac{d\vec{v}_{CG}}{dt} + \frac{d\vec{\omega}_F}{dt} \times \vec{r}_{P-CG} + \vec{\omega}_F \times \frac{d\vec{r}_{P-CG}}{dt} \tag{14}$$

$$\sum \vec{F}_B^p = m_p \frac{d\vec{v}_p}{dt} - \vec{F}_H^p \tag{15}$$

where, $\vec{v}_{CG}$ and $\vec{\omega}_F$ stand for the center-of-gravity velocity of floc and angular velocity of floc respectively. $\vec{F}_B^p$ represents force exerted by fluid on each bond of the primary particle *p*, and the net force is the sum of all these forces that particle *p* has with other primary particles. $\vec{F}_H^p$ is the hydrodynamic force acting on the primary particle *p*. The internal stresses are calculated in all the bonds between the primary particles in a floc using the above equations. An asphaltene floc breaks into smaller flocs when straining or shearing stresses exceed the internal bonding force. Only one bond between the primary particles of the floc is assumed to break at each time step. In other words, the floc will break from the location of the maximum exerted stress. The velocities of the new flocs are determined by the conservation of momentum.

d. Solution algorithm

The schematic presentation of the computational domain is illustrated in Figure 1. Periodic boundary condition (PBC) is adopted in inlet/outlet boundaries for both continuous and discrete phases. For the continuous phase, no-slip condition is considered at the wall, while velocity vectors are reflected across symmetry planes on the symmetry boundary. The particle-wall interactions are the same as particle-particle interactions, where the wall is assumed as an infinite-diameter sphere with no displacement. Additionally, a totally elastic collision of the particles with a virtual wall has been expected on a symmetry boundary.

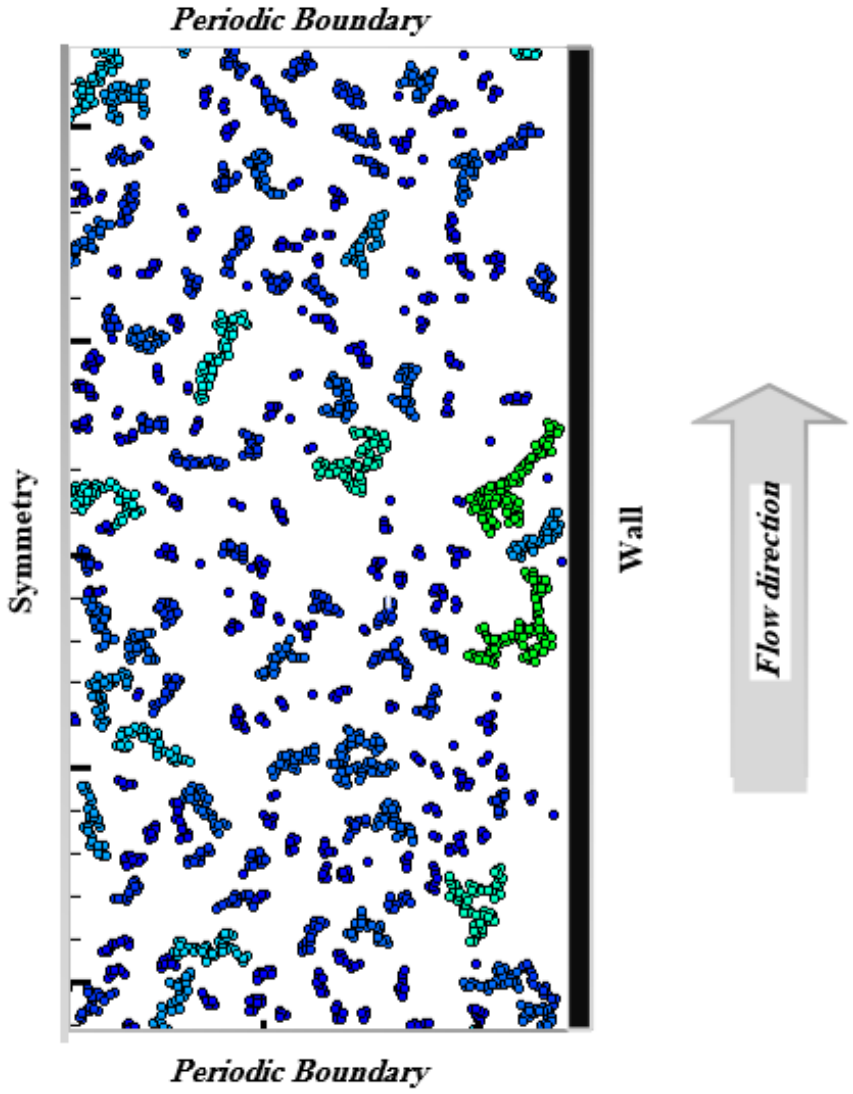

Figure 1

A schematic representation of the computational domain.

The workflow of the algorithm adopted to model asphaltene particle agglomeration and fragmentation is depicted in Figure 2. Initially, a defined number of primary particles are randomly distributed in the computational domain with no contact. The contact between particles is detected by the no-binary search (NBS) algorithm at each time step (Munjiza and Andrews, 1998). Then, the contact forces of colliding particles are calculated using a linear spring-dashpot model. A new floc will form if the attachment condition is fulfilled according to the coalescence model (the relative kinetic energy of two contacting asphaltene particles is greater than the energy barrier). The translational and angular velocities of the resultant floc are computed by the momentum conservation. Next, the drag force acting on particles as well as the drag force at each fluid cell is computed. In the following, the semi-implicit method for pressure-linked equations (SIMPLE) algorithm is used to solve the governing equations of the continuous phase (Patankar, 1980). After that, the positions and velocities of individual primary particles and flocs are updated on the basis of the computed contact and drag forces. Finally, the fragmentation of asphaltene flocs because of hydrodynamic shear forces is checked.

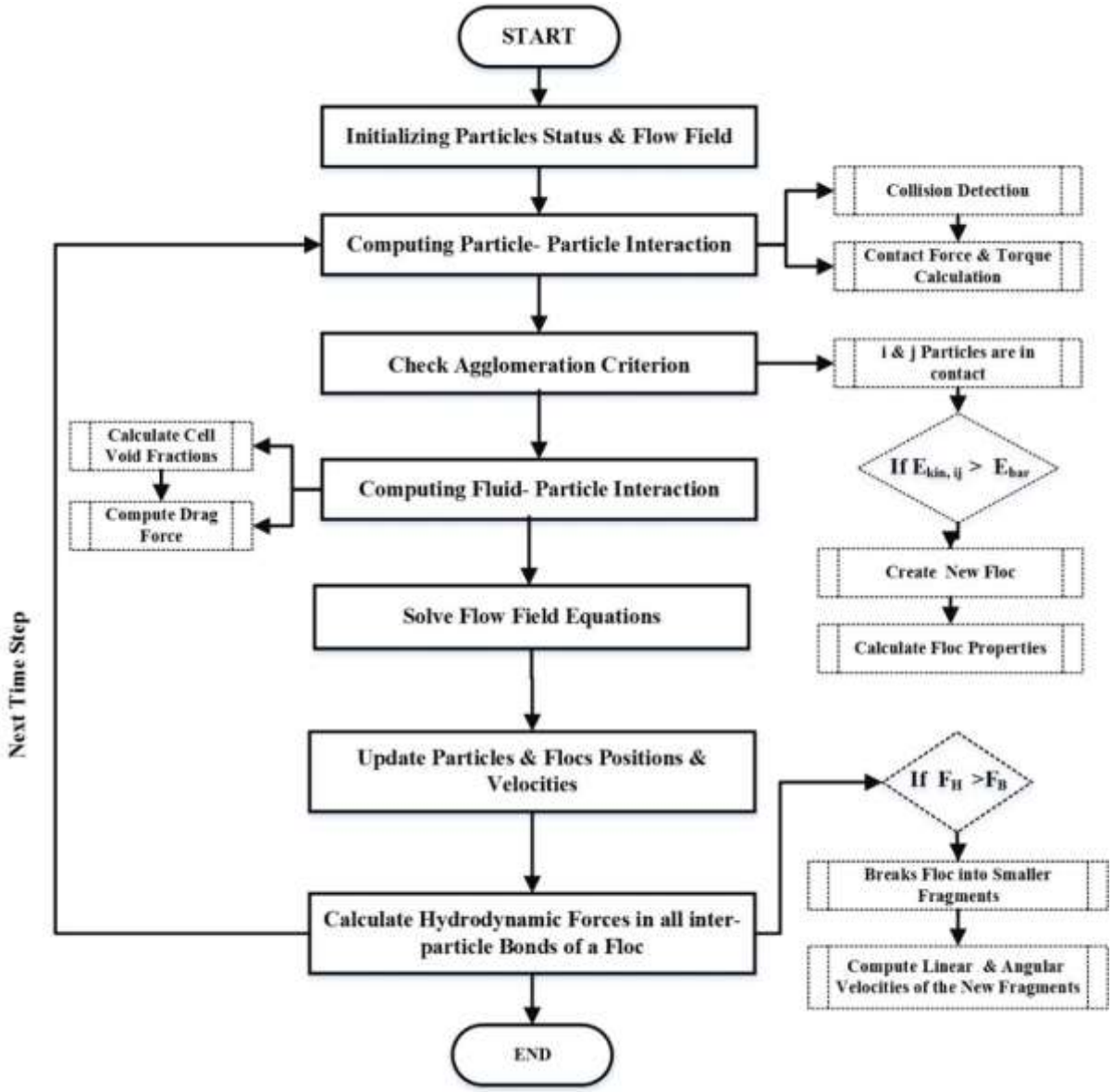

Figure 2

The workflow of the algorithm adopted to model asphaltene particle agglomeration and fragmentation.

The simulation parameters of the continuous and dispersed phases along with the size of computational domain are embedded in Table 2. The experimental results provided by Mohammadi et al. (Mohammadi et al., 2016) including asphaltene and solution solubility parameters along with experimental collision efficiencies are used to calculate the constants in Equation 13. The asphaltene and solution solubility parameters, temperature, the calculated values of the constants, and the energy barrier are tabulated in Table 3.

Table 2

Simulation parameters of the continuous and dispersed phases along with the size of computational domain.

Continuous phase (oil)		**Discrete phase (asphaltene particles)**		**Computational domain**		
Velocity (m/s)	0.75	Number of primary particles	5000	Width (m)	Height (m)	Thickness (m)
Density (kg.m^{-3})	607	Primary particle diameter (m)	1×10^{-6}	1.2×10^{-4}	7.2×10^{-4}	1×10^{-6}
Viscosity (kg.m^{-1}.s^{-1})	2.4×10^{-4}	Primary particle shape	Spherical			
Time step (s)	1×10^{-7}	Density (kg.m^{-3})	1200			
		Spring constant (N.m^{-1})	800			
		Sliding friction coefficient	0.64			
		Restitution coefficient	0.5			
		Time step (s)	1×10^{-10}			
		Bond strength (N)	2.76×10^{-7}			

Table 3

Parameters of the energy barrier equation according to Mohammadi et al. (2016).

δ_{asph} (Pa$^{0.5}$)	δ_{sol} (Pa$^{0.5}$)	T (K)	C_1	C_2	U_{bar} (N.m)
18620	9490	408	6.25×10^{8}	4.562	1.654×10^{-20}

2.2. Semi-analytical model

The number of particle-particle collisions per unit time per unit volume, N_C, for a system containing n_p uniformly sized primary particles of radius R_p under a laminar flow at a shear rate of γ has been derived by Levich (1962):

$$N_C = \frac{32}{3} {n_p}^2 {R_p}^3 \gamma \tag{16}$$

Accordingly, when floc fragmentation, because of hydrodynamic forces, is omitted, the rate of loss of flocs, n, with an equivalent radius of R_F is given by:

$$\frac{dn}{dt} = -\frac{32}{3} n^2 {R_F}^3 \gamma \beta \tag{17}$$

By replacing n in terms of R_F and integrating Equation 17, the change in floc radius with respect to time is obtained by (Hogg, 1987; Doraiswamy et al., 1996):

$$\frac{R_F}{R_p} = \exp\left(\frac{8\varphi\gamma\beta t}{3\pi}\right) \tag{18}$$

According to the above equation, in the absence of floc fragmentation, the equivalent radius of the flocs increases exponentially during the simulation. The fragmentation of flocs due to hydrodynamic forces limits the growth of the flocs, and eventually an equilibrium number density of flocs (the number of flocs per unit volume), n_{eq}, is reached. Equation 17 was modified to explain the effect of fragmentation on floc growth (Brown and Glatz, 1987):

$$\frac{dn}{dt} = -8\varphi\gamma\beta(n - n_{eq})\pi \tag{19}$$

Finally, Chimmili et al. (1998) have derived the following expression for the mean floc radius, R_F, as a function of time:

$$R_F = \frac{R_{eq}}{\left[1 + \left(\left(\frac{R_{eq}}{R_p}\right)^3 - 1\right)\exp(-\frac{8\varphi\gamma\beta t}{\pi})\right]^{\frac{1}{3}}} \tag{20}$$

3. Results and discussions

3.1. Simulation results

The flow field and the streamlines of fluid velocity in *x* and *y* directions at a certain time in the middle of the simulation are presented in Figure 3a and 3b respectively. The growth of asphaltene particles can be specified by the change in the normalized mean asphaltene floc radius (R_F/R_p) and average number of primary particles per floc ($n_{p\text{-}F}$), which are defined as follows (Rahmani et al., 2003; Zahnow et al., 2011):

$$\frac{\bar{R}_F}{R_p} = \frac{\sum_i (n_i \times R_{Fi})}{\sum_i n_i} / R_P \tag{21}$$

$$\bar{n}_{p-F} = \frac{\sum_i (n_{p-Fi} \times N_{Fi})}{N_F} \tag{22}$$

a) the fluid velocity in *x*-direction

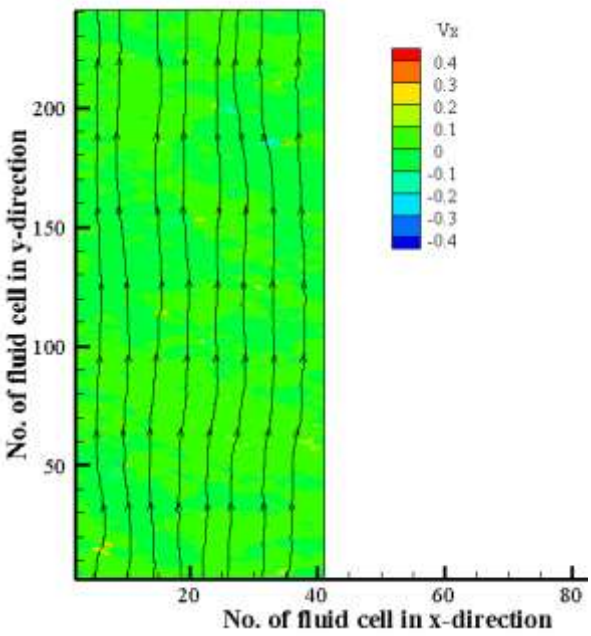

b) the fluid velocity in *y*-direction

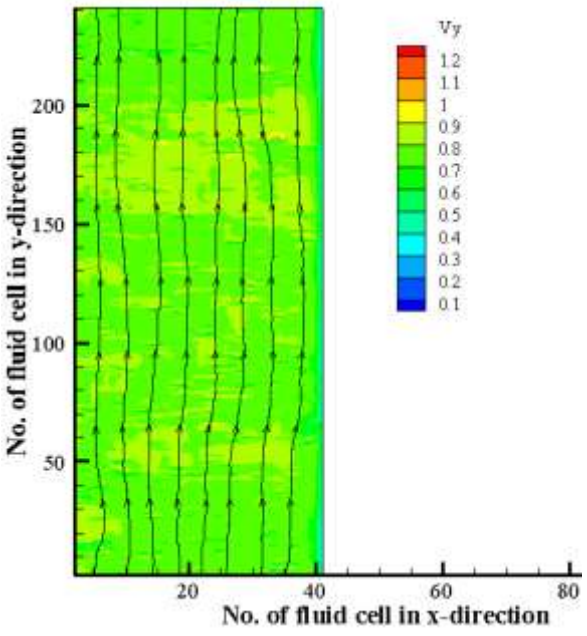

Figure 3

The flow field along with streamlines of fluid velocity in a) *x*-direction and b) *y*-direction.

The evolution of mean asphaltene floc radius is shown in Figure 4a. During asphaltene particle flocculation, mean floc size initially increases exponentially since the agglomeration is dominant. Then, the floc growth slows down since fragmentation becomes important; finally, the evolution of asphaltene flocs stops as a dynamic equilibrium is established between the agglomeration and fragmentation processes. Figure 4b illustrates the change in the average number of primary particles per floc; it approximately shows a trend similar to the evolution of mean floc radius.

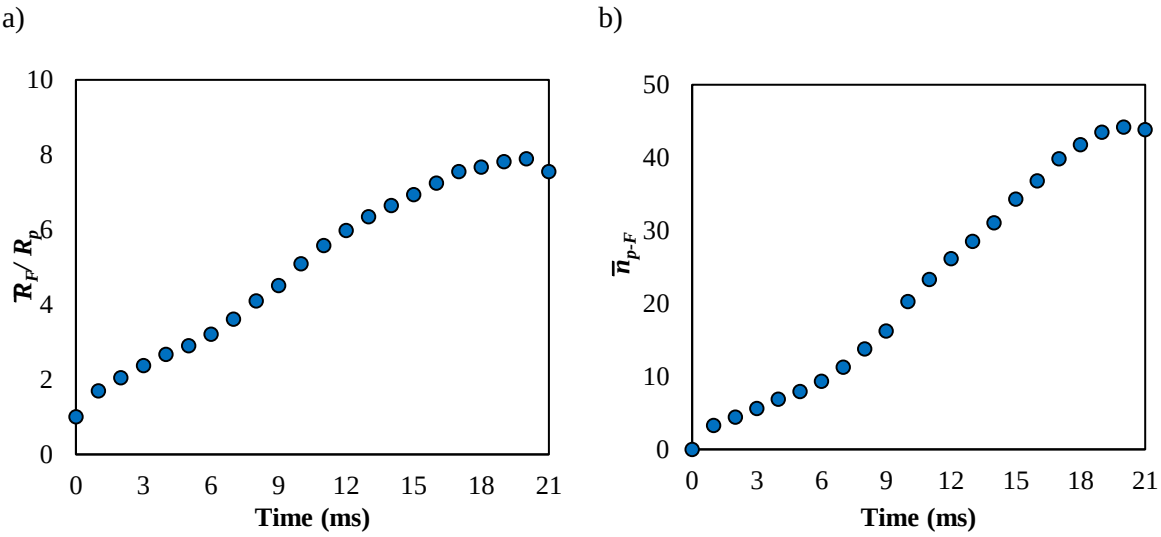

Figure 4

The evolution of a) mean asphaltene floc radius and b) the average number of primary particles per floc.

Figure 5 depicts the PSD's of asphaltenes at different simulation times. As expected, asphaltene PSD's move from fine to coarse sizes during the simulation. It should also be noted that the percentage of small asphaltene flocs is considerable even at the late time of evolution. It can be explained by the fragmentation of large flocs into smaller ones due to hydrodynamic forces. Consequently, the large asphaltene flocs have low frequencies at all the simulation times.

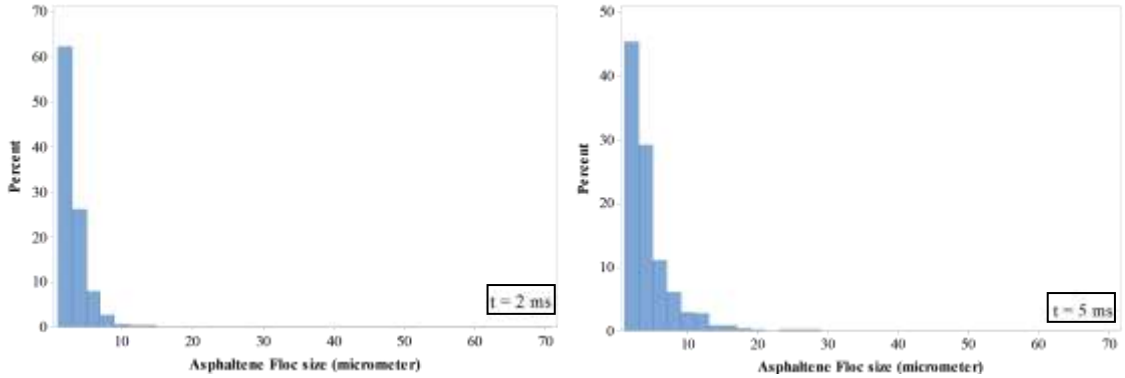

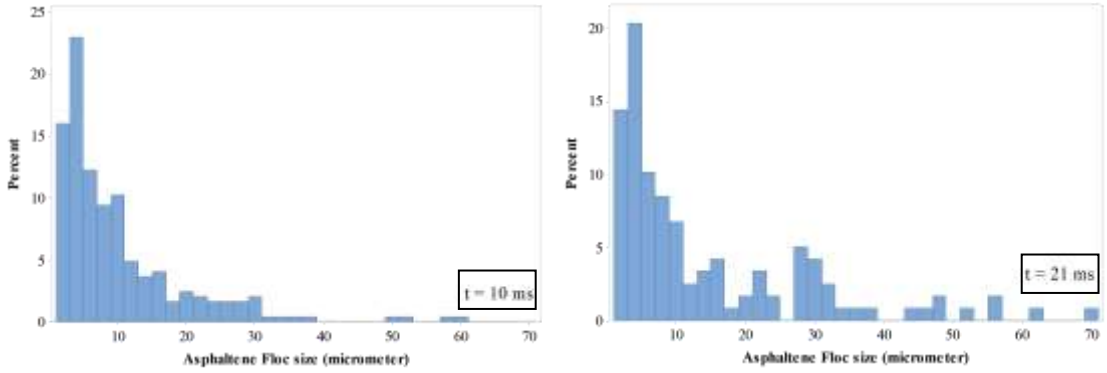

Figure 5

Distribution of asphaltene flocs at different simulation times.

Several probability distribution functions were examined to fit the asphaltene PSD results, and the log-normal distribution showed the best match, which agrees with the nature of asphaltene as mentioned in the previous studies (Ferworn et al., 1993; Rastegari et al., 2004). The log-normal distributions fitted with the PSD results at different simulation times are compared in Figure 6. Gradually, the percentage of small flocs decreases, and larger flocs are formed as a result of small floc agglomeration.

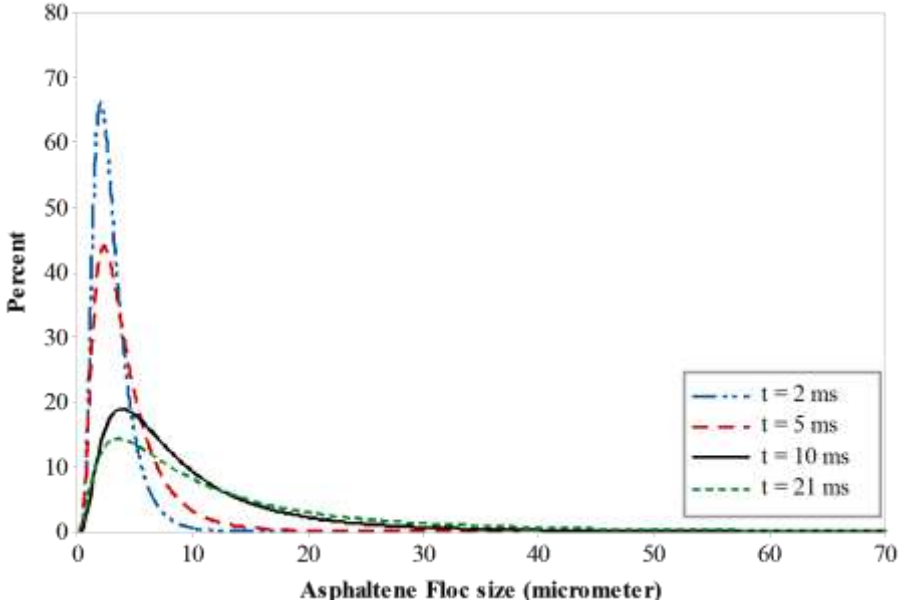

Figure 6

Comparison of the log-normal distributions fitted with the PSD results at different simulation times.

As stated in the related literature, the asphaltene flocs exhibit a fractal-like structure. Therefore, the average number of primary particles per floc is related to the mean asphaltene floc size by Equation 23 (Rastegari et al., 2004):

$$\bar{n}_{p-F} = k\left(\frac{\bar{R}_F}{R_p}\right)^{d_f} \tag{23}$$

To calculate the average fractal dimension, $\bar{n}_{p\text{-}F}$ is plotted versus $\bar{R}_F/R_p$ on a log-log scale, and d_f is obtained from the slope of the plot as demonstrated in Figure 7. As a result, the average fractal dimension of the asphaltene flocs equals 1.696, which agrees with the values reported in the literature (Dabir et al., 1996; Rastegari et al., 2004; Rahmani et al., 2005). The average fractal dimension indicates that the resultant asphaltene flocs have relatively open structures.

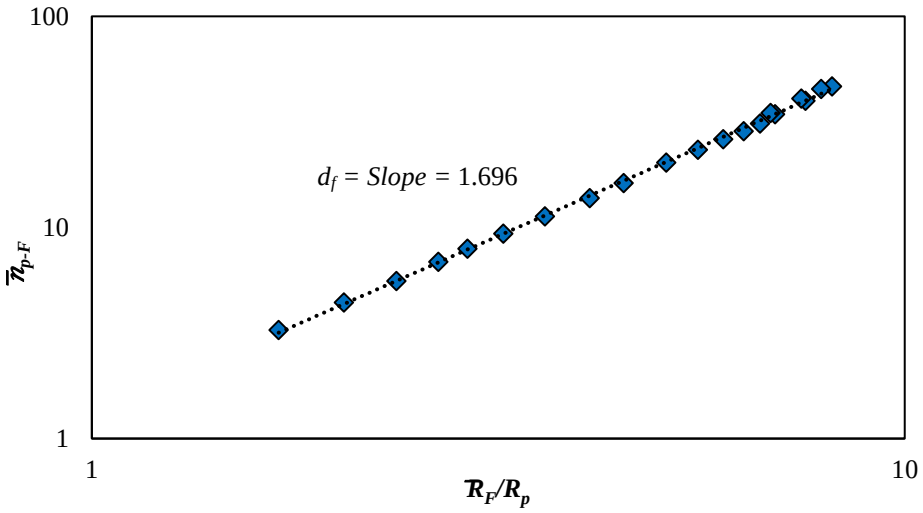

Figure 7

The average number of primary particles per floc versus mean asphaltene floc size.

3.2. Effect of fluid velocity on mean asphaltene floc size and structure

Figure 8 depicts the evolution of asphaltene flocs as a function of fluid velocity. When fluid velocity increases, it improves the rate of agglomeration and fragmentation processes. Subsequently, the dynamic equilibrium between the corresponding processes is reached more quickly. Additionally, since more fragmentation occurs at higher fluid velocities, the equilibrium mean floc radius is smaller.

a) b)

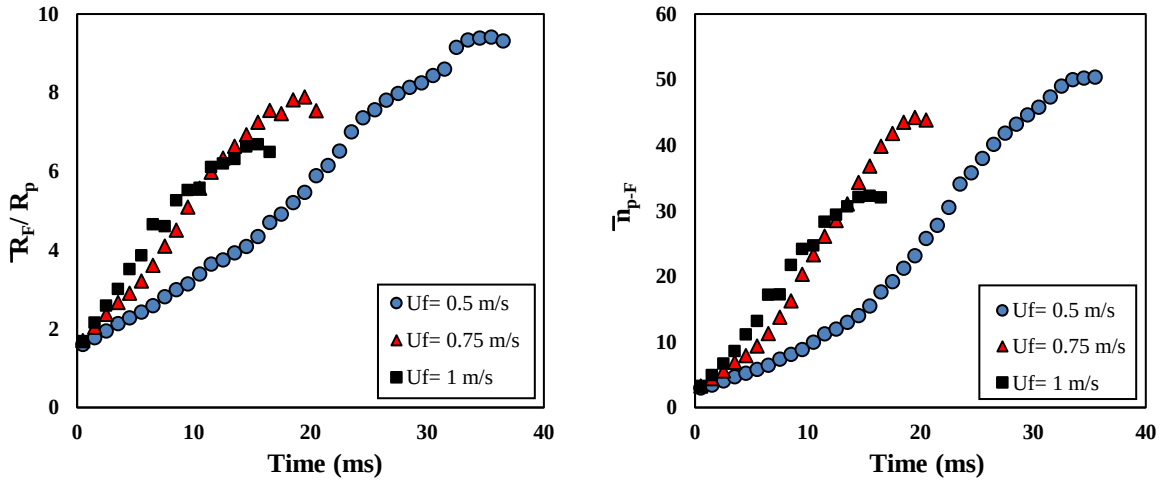

Figure 8

The evolution of a) mean asphaltene floc radius and b) the average number of primary particles per floc at different fluid velocities.

The lognormal distributions fitted with the PSD results of asphaltene flocs in a steady state condition at different fluid velocities are depicted in Figure 9. Asphaltene floc PSD's shift to smaller sizes within narrower ranges as fluid velocity rises.

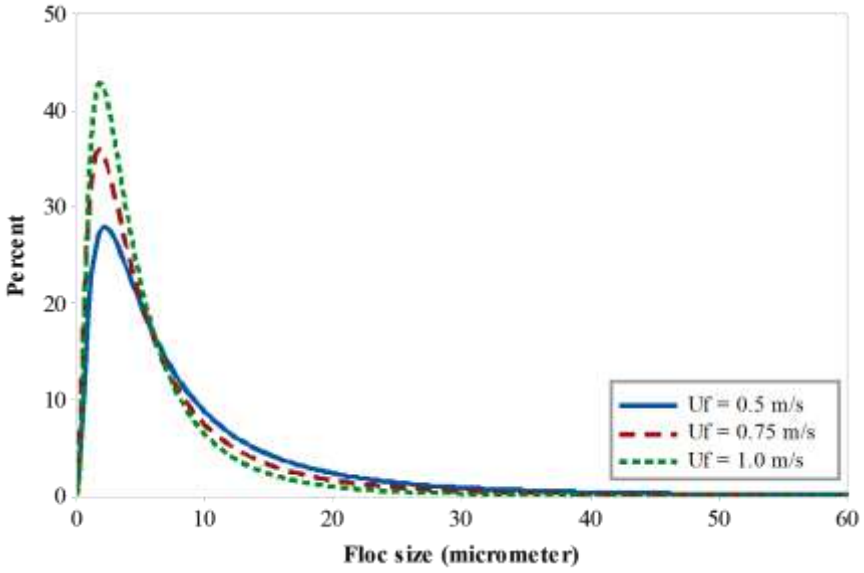

Figure 9

Comparison of the log-normal distributions fitted with the PSD results at different fluid velocities.

Figure 10 shows the average fractal dimension with respect to fluid velocity. The average fractal dimension rises by raising fluid velocity. Indeed, more fragmentations at higher fluid velocities result in smaller asphaltene flocs with more compact structures as seen in the PSD results.

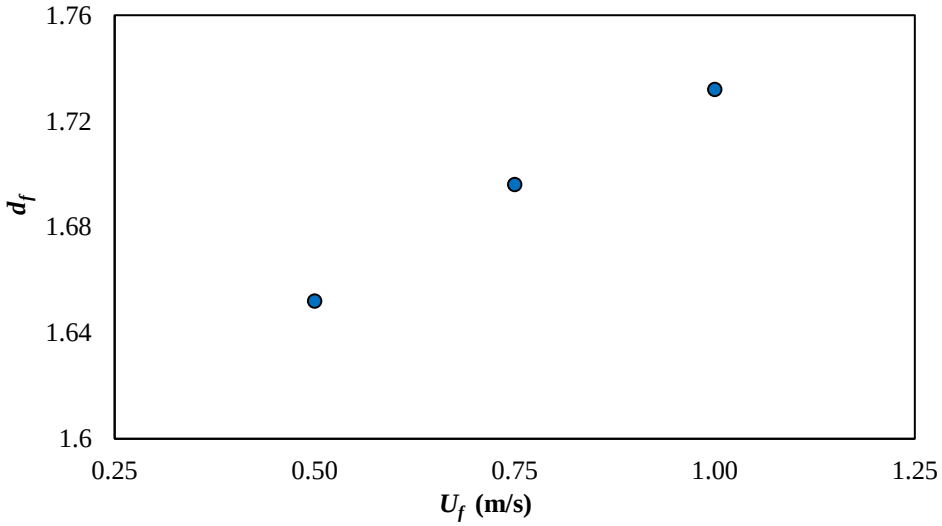

Figure 10

Average fractal dimension versus fluid velocity.

3.3. Comparison of the simulation results with semi-analytical model

The semi-analytical model was utilized to fit the temporal evolution of mean asphaltene floc radius at different fluid velocities resulted from the simulation (see Figures 11 to 13). At all the fluid velocities, the semi-analytical model underestimates the mean floc radius at early times, whereas it overestimates

the mean floc radius values at later times before a steady state is established. Generally, the semi-analytical model satisfactorily matches the simulation results.

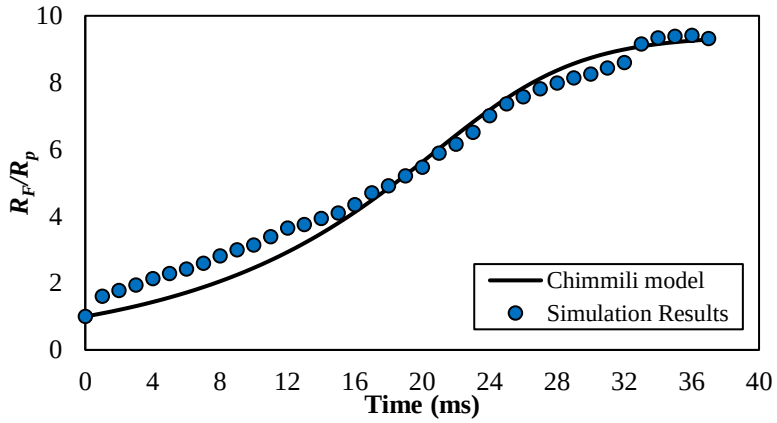

Figure 11

Comparison of the simulation asphaltene particles size and Chimmili's model at U_f = 0.5 m/s.

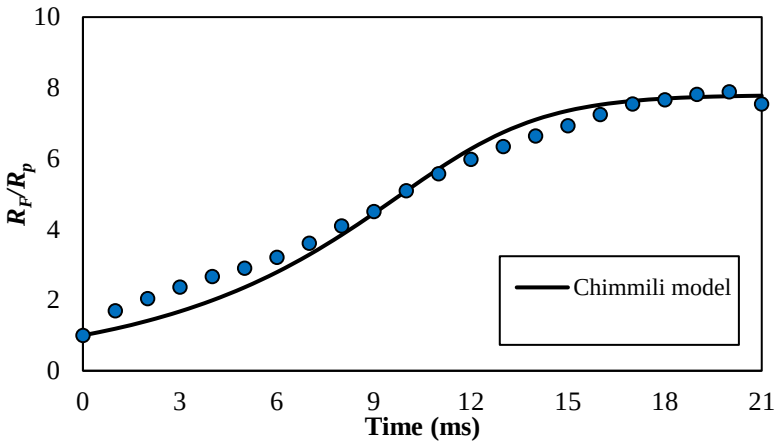

Figure 12

Comparison of the simulation asphaltene particles size and Chimmili's model at U_f = 0.75 m/s.

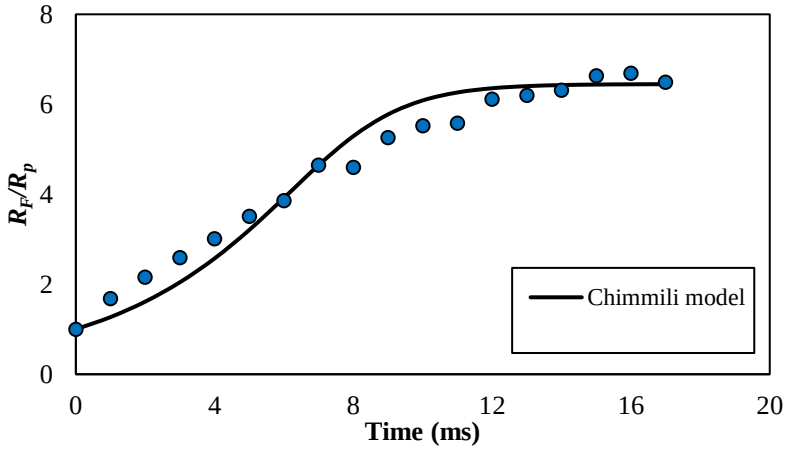

Figure 13

Comparison of the simulation asphaltene particles size and Chimmili's model at U_f = 1.0 m/s.

4. Conclusions

In this work, the kinetics of asphaltene flocculation was investigated using a DEM-CFD approach under a shear flow. DEM was used in combination with a new proposed coalescence model to describe the process of asphaltene particle agglomeration. The fragmentation of the resultant asphaltene flocs was also considered in response to hydrodynamic forces. Moreover, the asphaltene flocs were tracked as real objects with irregular shapes to account for the effect of floc structure on the corresponding processes. At early times, mean floc size increases exponentially in the absence of fragmentation, and, after that, fragmentation becomes important and limits the floc growth. Finally, a steady state condition is achieved due to a dynamic equilibrium between the agglomeration and fragmentation processes. Asphaltene PSD's also move from fine to coarse sizes during the evolution. The fragmentation of asphaltene flocs leads to the presence of a considerable number of small flocs at a later time of evolution. Log-normal distribution matches the PSD results best, which is also in agreement with asphaltene nature. Increasing fluid velocity establishes the steady state condition more quickly, so asphaltene flocs have smaller sizes and a higher fractal dimension in this condition. The PSD results illustrate the presence of smaller floc sizes at higher fluid velocities. The obtained average fractal dimensions are in the range of 1.65 to 1.74, which agrees with values reported in the literature. Finally, the semi-analytical model proposed by Chimmili et al. can suitably match the simulation results.

Nomenclatures

A_{cell}	Area of fluid cell (m^2)	U_{bar}	Energy barrier (N.m)
A_p	Area of primary particle (m^2)	U_f	Fluid velocity ($m.s^{-1}$)
C_1 , C_2	Constants of energy barrier equation	v_{ij}	Relative velocity of colliding particles *i* and *j*
C_D	Fluid drag coefficient	v_i	Translational velocity of particle, *i* ($m.s^{-1}$)
d_f	Mass fractal dimension	v_{CG}	Velocity of floc center of gravity ($m.s^{-1}$)
$E_{kin,\ ij}$	Relative kinetic energy of colliding particles (N.m)	V_p	Primary particle volume (m^3)
F^f_p	Particle–fluid interaction force (N)		
f_i	Drag force acting on particle in a fluid cell	**Greeks**	
F^n_{cont}	Normal contact force (N)	α^i_p	Fractional area of particle *i* in the fluid cell
F^p_B	Force exerted by fluid in each bond of the primary particle *p* (N)	β	Collision efficiency
F^p_H	Hydrodynamic force acting on the primary particle *p* (N)	γ	Shear rate
F^t_{cont}	Tangential contact force (N)	δ_{asph}	Asphaltenes solubility parameter ($Pa^{0.5}$)
g	Gravitational acceleration ($m.s^{-2}$)	δ_{sol}	Solution solubility parameter ($Pa^{0.5}$)
I_i	Particle, *i*, moment of inertia	ε	Porosity
k	Prefactor	η_n	Normal damping coefficient
k_B	Boltzmann's constant ($m^2\ kg\ s^{-2}\ K^{-1}$)	η_t	Tangential damping coefficient

k_n	Normal spring coefficient ($N.m^{-1}$)	μ_f	Fluid viscosity ($kg.m^{-1}.s^{-1}$)
k_t	Tangential spring coefficient ($N.m^{-1}$)	μ_p	Friction coefficient
m_i	Particle, i, mass (kg)	ξ_n	Normal overlap
N_C	Number of collisions	ξ_t	Tangential overlap
N_F	Number of asphaltene flocs	$\xi_{t,0}$	Tangential overlap in the previous time step
n	Number density of floc (m^{-3})	ρ_f	Fluid density ($kg.m^{-3}$)
n_{eq}	Equilibrium number density of floc (m^{-3})	τ	Fluid viscous stress tensor
n_{ij}	Normal unit vector of colliding particles i and j	φ	Particulate volume fraction
$n_{p\text{-}F}$	Number of primary particles in floc	ω_i	Angular velocity of particle, i (s^{-1})
$\overline{n}_{p\text{-}F}$	Average number of primary particles per floc	**Subscripts**	
P	Pressure (Pa)	F	Floc
$r_{cont,}$	A vector from the center of primary particle to the contact point	f	Fluid
$r_{p\text{-}CG}$	Distance of the primary particle p from the center of gravity of the floc	p	Primary particle
R_{eq}	Equilibrium mean asphaltene floc radius (m)		
$\overline{R}_F$	Mean asphaltene floc radius (m)		
R_p	Primary particle radius (m)		
T	Temperature (K)		
t_{ij}	Unit vector perpendicular to normal unit vector		

References

Anderson, T. B. and Jackson, R., Fluid Mechanical Description of Fluidized Beds: Equations of Motion, Ind. Eng. Chem. Fund., Vol. 6, p. 527-539, 1967.

Brown, D. L. and Glatz, C. E., Aggregate Breakage in Protein Precipitation, Chem. Eng. Sci., Vol. 42, p. 1831-1839, 1987.

Chimmili, S., Doraiswamy, D. and Gupta, R. K., Shear-induced Agglomeration of Particulate Suspensions, Ind. Eng. Chem. Res., Vol. 37, p. 2073-2077, 1998.

Cundall, P. A. and Strack, O. D., Discrete Numerical Model for Granular Assemblies, Geotechnique, Vol. 29, p. 47-65, 1979.

Doraiswamy, D., Gupta, R. K., and Chimmili, S., Particle Agglomeration and Migration Effects in Laminar Flow Systems, American Institute of Chemical Engineers, 1996.

Dabir, B., Nematy, M., and Mehrabi, A.R., Asphalt Flocculation and Deposition: III. The Molecular Weight Distribution, Fuel, Vol. 75, p. 1633–1645, 1996.

Daneshvar, S., Asphaltene Flocculation in Diluted Bitumen, M.S. Thesis, University of Calgary, 2005.

Ergun, S., Fluid Flow through Packed Columns, Chem, Eng. Prog., Vol. 48, p. 89–94, 1952.

Eskin, D., Ratulowski, J., Akbarzadeh, K., and Pan, S., Modelling Asphaltene Deposition in Turbulent Pipeline Flows, Can. J. Chem. Eng., Vol. 89, p. 421–441, 2011.

Eyssautier, J., Levitz, P., and Espinat, D., Insight into Asphaltene Nanoaggregate Structure Inferred by Small Angle Neutron and X-ray Scattering, J. Phys. Chem. B., Vol. 115, p. 6827–6837, 2011.

Fallahnejad G. and Kharrat R., Asphaltene Deposition Modeling during Natural Depletion and Developing a New Method for Multiphase Flash Calculation, Iranian Journal of Oil & Gas Science and Technology, Vol. 5, No. 2, p. 45-65, 2016.

Fenistein, D., Barré, L., and Broseta, D., Viscosimetric and Neutron Scattering Study of Asphaltene Aggregates in Mixed Toluene/Heptane Solvents, Langmuir, Vol. 14, p. 1013–1020, 1998.

Ferworn, K. A., Svrcek, W. Y., and Mehrotra, A. K., Measurement of Asphaltene Particle Size Distributions in Crude Oils Diluted with n-Heptane, Industrial & Engineering Chemistry Research, Vol. 32, No. 5, p. 955–959, 1993.

Haghshenasfard M. and Hooman K., CFD Modeling of Asphaltene Deposition Rate from Crude Oil, Journal of Petroleum Science and Engineering, Vol. 128, p. 24-32, 2015.

Haji-Akbari, N., Masirisuk, P., Hoepfner, M. P., and Fogler, H. S. A, Unified Model for Aggregation of Asphaltenes, Energy and Fuels, Vol. 27, p. 2497–2505, 2013.

Headen, T. F., Boek, E. S., Stellbrink, J., and Scheven, U. M., Small Angle Neutron Scattering (SANS and V-SANS) Study of Asphaltene Aggregates in Crude Oil, Langmuir, Vol. 25, p. 422-428, 2009.

Henry, C., Minier, J. P., Pozorski, J., and Lefèvre, G., A New Stochastic Approach for the Simulation of Agglomeration between Colloidal Particles, Langmuir, Vol. 29, p. 13694–13707, 2013.

Hoepfner, M. P., Vilas Boas Favero, C., Haji-Akbari, N., and Fogler, H. S., The Fractal Aggregation of Asphaltenes, Langmuir, Vol. 29, p. 8799–8808, 2013.

Hogg, R., Flocculation Phenomena in Fine Particle Dispersions, Ceramic Powder Sci., Vol. 21, p. 467-481, 1987.

Hoomans, B. P. B., Kuipers, J. A .M., Briels, W. J., and Van Swaaij, W. P. M., Discrete Particle Simulation of Bubble and Slug Formation in a Two-dimensional Gas-fluidized Bed: A Hard-Sphere Approach, Chemical Engineering Science, Vol. 51, p. 99–118, 1996.

Jamialahmadi M., Soltani B., Müller-Steinhagen H., and Rashtchian D., Measurement and Prediction of the Rate of Deposition of Flocculated Asphaltene Particles from Oil, International Journal of Heat and Mass Transfer, Vol. 52, p. 4624-34, 2009.

Khoshandam, A. and Alamdari, A., Kinetics of Asphaltene Precipitation in a Heptane-toluene Mixture, Energy and Fuels, Vol. 24, p. 1917–1924, 2010.

Kokal, S. L. and Sayegh, S. G., Asphaltenes: The Cholesterol of Petroleum, SPE 29787, p. 169–180, 1995.

Kruggel-Emden, H., Rickelt, S., Wirtz, S., and Scherer, V., A Study on the Validity of the Multi-sphere Discrete Element Method, Powder Technology, Vol. 188, p. 153–65, 2008.

Levich, V. G., Physicochemical Hydrodynamics, Prentice-Hall, 1962.

Maqbool, T., Raha, S., Hoepfner, M. P., and Fogler, H. S., Modeling the Aggregation of Asphaltene Nanoaggregates in Crude oil-precipitant Systems, Energy and Fuels, Vol. 25, p. 1585–1596, 2011.

Mason, T. G. and Lin, M. Y., Time-resolved Small Angle Neutron Scattering Measurements of Asphaltene Nanoparticle Aggregation Kinetics in Incompatible Crude Oil Mixtures, Journal of Chemical Physics., Vol. 119, p. 565–571, 2003.

Mohammadi, S., Rashidi, F., Mousavi-Dehghani, S. A., and Ghazanfari, M. H., Modeling of Asphaltene Aggregation Phenomena in Live Oil Systems at High Pressure-high Temperature, Fluid Phase Equilibria, Vol. 423, p. 55–73, 2016.

Munjiza, A. and Andrews, K. R. F., NBS Contact Detection for Similar Sizes, International Journal for Numerical Methods in Engineering, Vol. 149, p. 131–149, 1998.

Patankar, S. V., Numerical Heat Transfer and Fluid Flow, Hemisphere Publishing Corporation, 1980.

Rahmani, N. H. G., Dabros, T., and Masliyah, J. H., Fractal Structure of Asphaltene Aggregates, Journal

of Colloid and Interface Science - Elsevier, Vol. 285, p. 599–608, 2005.

Rahmani, N. H. G., Dabros, T., and Masliyah, J. H., Evolution of Asphaltene Floc Size Distribution in Organic Solvents under Shear, Chemical Engineering Science, Vol. 59, p. 685–697, 2004.

Rahmani, N. H. G., Masliyah, J., H., Dabros, T., Characterization of Asphaltenes Aggregation and Fragmentation in a Shear Field, AIChE J., Vol. 49, p. 1645–1655, 2003.

Ramirez-Jaramillo E., Lira-Galeana C., and Manero O., Modeling Asphaltene Deposition in Production Pipelines, Energy and Fuels, Vol. 20, No. 3, p.1184-96, 2006.

Rastegari, K., Svrcek, W. Y., and Yarranton, H. W., Kinetics of Asphaltene Flocculation, Industrial & Engineering Chemistry Research, Vol. 43, p. 6861–6870, 2004.

Salimi F., Ayatollahi S., and Vafaie Seftie M., An Experimental Investigation and Prediction of Asphaltene Deposition during Laminar Flow in the Pipes Using a Heat Transfer Approach, Iranian Journal of Oil & Gas Science and Technology, Vol. 6, No. 2, p.17-32, 2017.

Savvidis, T. G., Fenistein, D., Barr, L., and Bhar, E., Aggregated Structure of Flocculated Asphaltenes, AIChE J., Vol. 47, p. 206–211, 2001.

Schutte, K. C. J., Portela, L. M., Twerda, A., and Henkes, R. A. W. M., Hydrodynamic Perspective on Asphaltene Agglomeration and Deposition, Energy and Fuels, Vol. 29, p. 2754–2767, 2015.

Seyyedbagheri, H. and Mirzayi, B., Eulerian Model to Predict Asphaltene Deposition Process in Turbulent Oil Transport Pipelines, Energy & Fuels, Vol. 31, No. 8, p. 8061-71, 2017.

Sheu, E., Long, Y., and Hamza, H., Asphaltene Self-association and Precipitation in Solvents-AC Conductivity Measurements, in Asphaltenes, Heavy Oils, and Petroleomics, Springer, New York, 2007.

Shirdel M., Paes D., Ribeiro P., and Sepehrnoori K., Evaluation and Comparison of Different Models for Asphaltene Particle Deposition in Flow Streams, Journal of Petroleum Science and Engineering, Vol. 84, p. 57-71, 2012.

Solaimany-Nazar, A. R. and Rahimi, H., Dynamic Determination of Asphaltene Aggregate Size Distribution in Shear Induced Organic Solvents, Energy and Fuels, Vol. 22, p. 3435–3442, 2008.

Solaimany-Nazar, A. R. and Rahimi, H., Investigation on Agglomeration-fragmentation Processes in Colloidal Asphaltene Suspensions, Energy and Fuels, Vol. 23, p. 967–974, 2009.

Wen, C. Y. and Yu, Y. H., Mechanics of Fluidization, Chemical Engineering Progress Symposium Series, Vol. 162, p. 100–111, 1966.

Xu, B. H. and Yu, A. B., Numerical Simulation of the Gas-solid Flow in a Fluidized Bed by Combining Discrete Particle Method with Computational Fluid Dynamics, Chemical Engineering Science, Vol. 52, p. 2785-2809, 1997.

Zahnow, J. C., Maerz, J., and Feudel, U., Particle-based Modeling of Aggregation and Fragmentation Processes: Fractal-like Aggregates, Physica D: Nonlinear Phenomena, Vol. 240, p. 882–893, 2011.